Landscape structure and climate influences on hydrologic response

Fabian Nippgen,[1] Brian L. McGlynn,[1] Lucy A. Marshall,[1] and Ryan E. Emanuel[2]

Received 19 July 2011; revised 5 October 2011; accepted 30 October 2011; published 20 December 2011.

[1] Climate variability and catchment structure (topography, geology, vegetation) have a significant influence on the timing and quantity of water discharged from mountainous catchments. How these factors combine to influence runoff dynamics is poorly understood. In this study we linked differences in hydrologic response across catchments and across years to metrics of landscape structure and climate using a simple transfer function rainfall-runoff modeling approach. A transfer function represents the internal catchment properties that convert a measured input (rainfall/snowmelt) into an output (streamflow). We examined modeled mean response time, defined as the average time that it takes for a water input to leave the catchment outlet from the moment it reaches the ground surface. We combined 12 years of precipitation and streamflow data from seven catchments in the Tenderfoot Creek Experimental Forest (Little Belt Mountains, southwestern Montana) with landscape analyses to quantify the first-order controls on mean response times. Differences between responses across the seven catchments were related to the spatial variability in catchment structure (e.g., slope, flowpath lengths, tree height). Annual variability was largely a function of maximum snow water equivalent. Catchment averaged runoff ratios exhibited strong correlations with mean response time while annually averaged runoff ratios were not related to climatic metrics. These results suggest that runoff ratios in snowmelt dominated systems are mainly controlled by topography and not by climatic variability. This approach provides a simple tool for assessing differences in hydrologic response across diverse watersheds and climate conditions.

Citation: Nippgen, F., B. L. McGlynn, L. A. Marshall, and R. E. Emanuel (2011), Landscape structure and climate influences on hydrologic response, *Water Resour. Res.*, *47*, W12528, doi:10.1029/2011WR011161.

1. Introduction

[2] Catchment structure (topography, geology, vegetation and soil patterns) has long been recognized as a first-order control for soil moisture [*Burt and Butcher*, 1985; *Western et al.*, 1999], hydrologic response [*Dunne and Black*, 1970; *Jencso et al.*, 2009; *Quinn et al.*, 1991] and biogeochemical processes [*Pacific et al.*, 2011; *Riveros-Iregui and McGlynn*, 2009] in forested mountain landscapes. At the same time, the impact of climatic variability on hydrologic processes and water resources has been intensively studied across various temporal and spatial scales [e.g., *Montgomery et al.*, 1997; *Nijssen et al.*, 2001; *Niehoff et al.*, 2002]. However, the extent to which the intersection of landscape structure and climatic variability influences hydrologic response and the timing of streamflow remains largely unknown. This raises the question: Do climate variability and landscape characteristics explain differences in the hydrologic responses among catchments?

[3] A parsimonious way to assess the response of catchments is through the use of transfer function models, which often utilize only rainfall and catchment runoff. Transfer functions are quantitative filters that describe the translation of a measured input (e.g., snowmelt/rainfall) into an output (e.g., runoff). In hydrology, transfer function models have been used to model solute transport through porous media [*Beven and Young*, 1988; *Jury*, 1982; *Maloszewski and Zuber*, 1982], river solute transport [*Wallis et al.*, 1989] and tracer residence time modeling and hydrograph separation [*Hrachowitz et al.*, 2009; *McGuire et al.*, 2002; *Weiler et al.*, 2003]. Rainfall-runoff applications of transfer functions date back to the unit hydrograph and its adaptations [*Dooge*, 1959; *Sherman*, 1932] where an amount of excess rainfall (i.e., effective rainfall) is convoluted with the unit hydrograph and thus translated into catchment runoff. Transfer function approaches usually assume linear behavior between rainfall amount and the resulting runoff, but they can contain nonlinear modules, as for the calculation of effective precipitation [*Jakeman and Hornberger*, 1993]. Transfer functions allow for qualitative and quantitative analysis of the integrated processes in catchments that translate inputs signals into output signals, subsuming complex catchment characteristics into one parsimonious function. Runoff transfer functions may differ among different catchments, and even for a single catchment the transfer function may differ through time.

[4] In this study we use a simple transfer function rainfall-runoff model (modified from TRANSEP, see *Weiler et al.* [2003]) to estimate mean response times. Mean

[1]Department of Land Resources and Environmental Sciences, Montana State University, Bozeman, Montana, USA
[2]Department of Forestry and Environmental Resources, North Carolina State University, Raleigh, North Carolina, USA

Copyright 2011 by the American Geophysical Union.
0043-1397/11/2011WR011161

hydrologic response time is a measure of how long it takes to discharge an amount of water equal to an effective precipitation input. Mean response time should not be confused with mean residence time (or mean transit time), terms that are often used in tracer based catchment modeling. Though seemingly similar, they are two very different metrics of catchment hydrology. Mean response time as it is used in this paper, refers to the transmission of an input magnitude or pressure response, while mean residence or transit time refers to the transmission of the water molecules themselves and not the pressure response. A mean residence time describes how long an individual water input (or molecule) remains in the catchment, while mean response time does not contain information about the age of water.

[5] Using this simple transfer function model, we examine how catchment structural characteristics and climatic variability affect the hydrologic response of mountain catchments. We examined runoff and precipitation data from seven adjacent catchments located in the mountains of central Montana over a 12 year period in conjunction with ten landscape metrics derived from high-resolution lidar data.

[6] Focus on adjacent catchments reduces confounding factors typically encountered when comparing catchments across regions. The close proximity and similar elevation range of the catchments also limit hydrologic process differences and rainfall/snow variability. Differences in transfer functions and the resulting mean response times are therefore signatures that we expect to be related to distinct catchment characteristics including structure and climate. We address the following questions in this study: (1) What is the role of landscape structure in determining intercatchment differences in mean response time?; (2) Can intracatchment (i.e., annual) variability in mean response time be explained by climate variability?

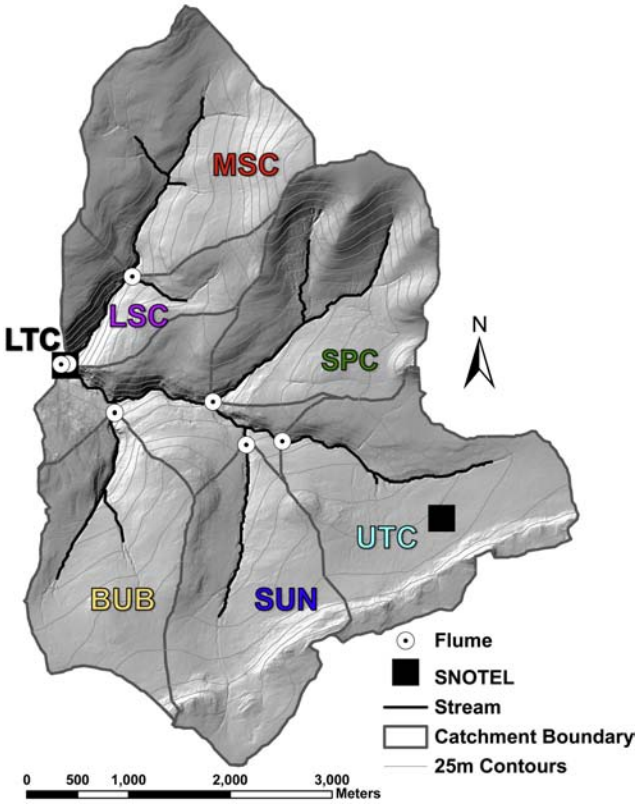

Figure 1. Tenderfoot Creek Experimental Forest with two SNOTEL sites and seven gauged catchments. The color coding remains the same for following figures. LTC, Lower Tenderfoot Creek; LSC, Lower Stringer Creek; MSC, Middle Stringer Creek; SPC, Spring Park Creek; UTC, Upper Tenderfoot Creek; SUN, Sun Creek; BUB, Bubbling Creek.

2. Methods

2.1. Site Description

[7] The Tenderfoot Creek Experimental Forest (TCEF) is located in the Lewis and Clark National Forest, which is part of the Little Belt Mountains in the Northern Rocky Mountains of central Montana (lat. 56.55′N, long. 110.52″W). The total area of TCEF encompasses 2300 ha and includes seven gauged catchments, Bubbling Creek (BUB), Lower Stringer Creek (LSC), Middle Stringer Creek (MSC), Lower Tenderfoot Creek (LTC), Spring Park Creek (SPC), Sun Creek (SUN) and Upper Tenderfoot Creek (UTC), with subcatchments ranging in size from 318 ha to 554 ha (Figure 1). Tenderfoot Creek is a headwater of the Smith River that drains into the Missouri River. In all subcatchments the slope generally increases downstream with more constrained and smaller riparian areas in a downstream direction. Rock outcrops and steep talus slopes are most frequent on lower portions of the catchment.

[8] The dominant tree species is lodgepole pine (*Pinus contorta*), though the forest also includes subalpine fir (*Abies lasiocarpa*), Engelmann spruce (*Picea engelmannii*) and whitebark pine (*Pinus albicaulis*). Shrubs and grasses dominate the riparian areas, which make up about 14% of the study area. Two of the subcatchments, SPC and SUN, were partially clearcut between 1999 and 2001 to investigate the effect of different silvicultural treatments on water yield and sediment export. Each watershed included two different types of treatments: In one treatment the forest was thinned and in the other treatment individual groups of trees were left standing with clearcut corridors between them; both treatment types removed approximately 50% of the tree basal area with total treated area of ∼127 ha in SPC (∼32% of the catchment area) and ∼162 ha in SUN (∼45% of the catchment area).

[9] Soils at TCEF are loamy Typic Cryochrepts located along hillslope positions and clayey Aquic Cryoboralfs in riparian zones and parks [*Holdorf*, 1981]. Watershed soils are 0.5–2 m deep. Average soil depths were found to be approximately 1 m, based on the installation of >180 shallow groundwater wells and soil pits located on hillslopes and in riparian areas [*Jencso et al.*, 2009].

[10] The most dominant geologic layer is Flathead Sandstone. Granite gneiss underlies the sandstone and is prevalent toward the bottom of the watersheds. The highest elevations of LSC and SPC are underlain by biotite hornblende quartz monzonite, which lies over a layer of shale (Wolsey formation). The sandstone portions of TCEF tend

to have a gentler slope whereas the other formations generally coincide with steeper slopes.

[11] Climate at TCEF is predominantly continental. For the 1961–1990 base period annual precipitation was about 880 mm [*Farnes*, 1995]. Approximately 70% of the precipitation volume falls as snow. Discharge usually peaks between mid-April and the end of May. Stream discharge peaks are generated by snowmelt and rain on snow events during the spring melt period. Discharge typically reaches its minimum in late September or October.

2.2. Landscape Analysis

[12] Topographic variables were derived from 1 m resolution airborne laser swath mapping (ALSM) data. The ALSM based digital elevation model (DEM) was resampled to 10 m, a resolution high enough to capture the actual topography but coarse enough not to introduce errant behavior due to micro topographical features such as fallen trees or individual boulders [see *Jencso et al.*, 2009].

[13] We calculated catchment-wide means and medians for 10 different landscape variables (Table 1). Topographic variables were derived from the 10 m DEM, whereas tree height (TH) was calculated by subtracting the last return LIDAR coverage (bare earth) from the first returns (elevation of canopy) [see *Emanuel et al.*, 2010]. Tree heights of up to 2 m were then resampled to 0 m to avoid noise caused by riparian vegetation and clear cut regrowth. Two sample nonparametric Kolmogorov-Smirnov tests were performed on pairs of watersheds to test for significant differences between entire distributions of landscape variables, while Kruskal-Wallis tests were performed on all seven watersheds to test for significant differences in the medians of landscape variable distributions.

[14] To assess interdependency among the landscape metrics, we also calculated a cross-correlation matrix for Lower Tenderfoot Creek (LTC) with Pearson's correlation coefficients for all landscape metrics with distinct values for each grid cell. Since TH was calculated based on the original 1 m resolution LIDAR data, the remaining variables were resampled from 10 m resolution to 1 m resolution in order to correlate them with the 1 m TH coverage. The correlations are based on more than 20,000,000 grid cells for each landscape variable.

2.3. Hydrologic Measurements

[15] Precipitation and discharge data were available for years 1996–2002 and 2005–2009. The model simulation period was from 1 March to the last day of February of the following year instead of the conventional water year (e.g., year 1996 runs from 1 March 1996 to 28 February 1997). This time period was selected to match the characteristic timing of annual snowmelt and the event-based nature of transfer function models, including a short "warm up" period and a longer time following the annual event. Discharge for the years 1996 through 2005 was made available by the USDA Forest Service. Discharge for the period 1996 through 2001 was available in daily time steps. For the years 2002 and 2005, stage was recorded every 15 min at H-Flumes or Parshall Flumes located at the catchment outlets using a high-precision potentiometer (model 3540, Bourns Inc., Riverside, CA) and later aggregated to a daily time series. The USDA obtained missing data for individual catchments and years by regression with other catchments. Data for the entire melt period was missing for the following watersheds and years: UTC 1997, SUN 2000 and UTC 2000. Small portions (∼15%) of the falling limb of the hydrograph were missing for SPC 2001, BUB 2001 and LTC 2001, small portions (∼10%) of the rising limb of the hydrograph were missing for SUN 1997, MSC 1998 and LTC 1998. For the years 2006 through 2010, stage was recorded every 30 min at the same flumes using capacitance rods with ±1 mm resolution (TruTrack Inc., Christchurch, New Zealand) and later aggregated to a daily time series. Precipitation and snowmelt were measured at two Natural Resources Conservation Service (NRCS) SNOTEL stations, one at Onion Park (2259 m) near the headwaters of UTC and the other at Stringer Creek near the bottom of the Experimental Forest next to the LSC flume (1996 m). The calculations of liquid water input (comprising snowmelt and rainfall) at the surface are based on four assumptions: (1) when both cumulative precipitation and SWE increase, neither melt nor liquid precipitation is occurring,

Table 1. Landscape Metrics Used in the Analysis With Their Abbreviations and Definitions

Landscape Metric	Abbreviation	Definition
Slope (°)	SLP	Slope of a grid cell based on the greatest elevation difference with its eight neighboring cells
Convergence (%)	CON	Convergence or divergence of a grid cell using the surrounding eight cells; 100% convergence means all surrounding grid cells flow into the center cell, 100% divergence means all surrounding cells face away from the center cell [after *Moore et al*., 2001]
Distance from creek (m)	DFC	The distance from a grid cell to the stream along a flow path
Gradient to creek (−)	GTC	The gradient of a flow path
Local input (ha)	LI	Upslope accumulated area (UAA) of a grid cell bordering the stream [*Grabs et al*., 2010; *Seibert and McGlynn*, 2007]
Hillslope power (−)	HP	UAA of a grid cell multiplied by the slope of the contributing area
Riparian buffering (−)	RP	Ratio of riparian area to hillslope area [*McGlynn and Seibert*, 2003]
Tree height (m)	TH	Average pixel elevation (tree height) above ground surface including the silvicultural treatment areas, calculated by subtracting the last return from the first return LIDAR coverage
Potential solar insolation (kWh m^{-2} yr^{-1})	INS	Potential annual solar insolation calculated for each grid cell [*Böhner and Antonic*, 2009]
Geology	GEO	Different geologic strata [*Reynolds and Brandt*, 2006]

(2) when SWE decreases and cumulative precipitation stays the same, melt is occurring, (3) when cumulative precipitation increases and SWE decreases, both melt and rain are occurring and finally (4) when SWE is 0 and cumulative precipitation increases, rain is occurring. We then subtracted SWE from cumulative precipitation. This can be expressed mathematically as

$$\frac{dI}{dt} = \begin{cases} 0, \ \frac{dP}{dt} > 0 \ \cap \ \frac{dS}{dt} > 0 \\ -\frac{dS}{dt}, \ \frac{dP}{dt} = 0 \ \cap \ \frac{dS}{dt} < 0 \\ \frac{dP}{dt} - \frac{dS}{dt}, \ \frac{dP}{dt} > 0 \ \cap \ \frac{dS}{dt} < 0 \\ \frac{dP}{dt}, \ \frac{dP}{dt} > 0 \ \cap \ S = 0 \end{cases}, \quad (1)$$

where I is the amount of liquid water input to the ground, P is cumulative precipitation (both liquid and solid), S is snow water equivalent, and t the time step. Note that a reduction of S results in the release of melt water from the snow pack.

[16] This results in a time series of cumulative liquid input, the numerical differentiation of which yields an input per unit time. Precipitation and snowmelt data were aggregated from 6 h time steps to a daily time series. Based on observed differences in precipitation and SWE of up to 20% between the two SNOTEL stations, we weighted and combined the input of the two SNOTEL sites by elevation. We calculated a linear regression for the elevation range between the Stringer and Onion Park SNOTEL sites and assigned each DEM grid cell a precipitation value based on the regression. All elevations >2259 m were assigned the Onion Park precipitation. Since TRANSEP is a lumped model the semidistributed precipitation was then averaged to a single value per time step for each catchment. In addition total SWE was calculated for the Onion Park and Stringer Creek SNOTEL sites for each of the 12 years. Maximum precipitation and snowmelt intensities were calculated with a moving average from one to 21 days.

2.4. Uncertainties Associated With the Use of Two SNOTEL Sites

[17] Calculating response times to determine differences between the catchments requires exact input time series for each of the catchments. An important assumption for the analysis is that differences in snow accumulation, the timing of melt and the magnitude of melt rates are adequately reflected by the elevation weighting employed based on the two SNOTEL sites. This is a strong but necessary assumption due to the limitation to two precipitation measurement sites. Multiple factors could play a role in determining SWE characteristics across the landscape. However, we believe that the elevation weighted input adequately describes the snow accumulation and melt timing differences between the catchments. *Smith and Marshall* [2010] quantified uncertainties for a predictive runoff model for TCEF and found that elevation had a greater impact on both runoff and melt than aspect. Personal observations of the authors over the course of six winters corroborate the assumption that elevation has a greater impact on snow accumulation than aspect. In addition, the SNOTEL sites are usually located on flat ground, not "favoring" a certain aspect. We acknowledge that aspect could lead to slight differences in the onset of snowmelt. However, considering the duration of the whole melt period this initial uncertainty is likley negligible. The general spatial variability of precipitation is, in our opinion, of less concern in contrast to convective summer rain storm events, which can be small in extent and therefore highly localized. Frontal snow storms at TCEF are usually of a greater spatial extent and easily cover the full extent of the experimental forest.

2.5. Hydrologic Model

[18] We used a simple rainfall-runoff transfer function model, a module of the Transfer Function Hydrograph Separation Model (TRANSEP) developed by *Weiler et al.* [2003]. A transfer function translates a measured input (effective daily rainfall + snowmelt) into an output (daily discharge) (Figure 2).

[19] The rainfall-runoff module in TRANSEP includes a nonlinear loss function, $s(t)$, to first transform measured precipitation into effective precipitation [*Jakeman and Hornberger*, 1993]:

$$s(t) = b_1 p(t) + (1 - b_2^{-1}) s(t - \Delta t), \quad (2)$$

$$s(t = 0) = b_3, \quad (3)$$

$$p_{\text{eff}}(t) = p(t) s(t), \quad (4)$$

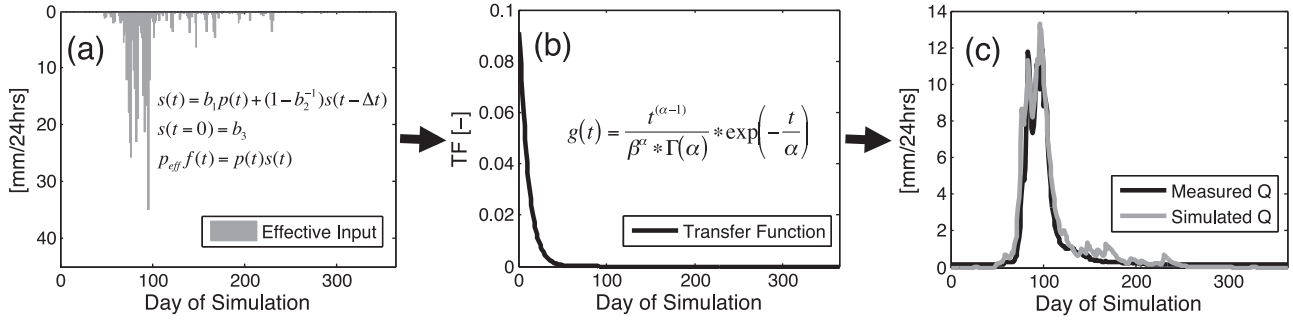

Figure 2. Flowchart representation of model implementation: (a) A measured input is transformed into effective precipitation by the loss function; (b) convolution of a calibrated transfer function and the effective precipitation results in (c) discharge. For our study, the parameters of the loss function and the parameters of the transfer function were optimized in 150,000 Monte Carlo simulations.

where $s(t)$ is the antecedent precipitation index, b_1 maintains the water balance that the total effective precipitation equals the total runoff, b_2 determines the rate at which the watershed dries out, b_3 sets the initial state of catchment wetness at the beginning of the time series, p_{eff} the effective precipitation and $p(t)$ is the measured rainfall and snowmelt input at time t.

[20] We applied the gamma distribution transfer function to daily data

$$g(\tau) = \frac{\tau^{\alpha-1}}{\beta^{\alpha}\Gamma(\alpha)} \exp\left(-\frac{\tau}{\alpha}\right), \tag{5}$$

where $g(\tau)$ is the value of the transfer function at a given lag time between rainfall and runoff, $\Gamma(\alpha)$ is the gamma function, α is the shape parameter and β a scale parameter. Multiplying α and β yields the mean value of the gamma distribution [*Kirchner et al.*, 2000], which can be interpreted as the mean response time. Therefore mean response time is defined as the average time that it takes for a given amount of water input (liquid precipitation and/or snowmelt) to leave the catchment through the outlet. The two-parameter gamma function was selected for our analysis as it is more flexible than an exponential function [*Hrachowitz et al.*, 2010] but does not require an additional splitting parameter as, for example, the two-parallel-linear-reservoir transfer function.

[21] The parameters in equations (2) and (5) were calibrated with 150,000 Monte Carlo simulations. Convolution of the transfer function (5) and the effective precipitation (2) results in runoff:

$$Q(t) = \int_0^t g(\tau) p_{\text{eff}}(t-\tau) d\tau, \tag{6}$$

where $Q(t)$ is the runoff at time t.

[22] Correlations between TRANSEP calculated mean response times and the catchment-averaged landscape and annual climatic variables were calculated as Pearson correlation coefficients. The means and medians of the landscape variables were tested for significant correlation with the catchment averages of mean response times (each catchment averaged over the 12 years of simulation). In addition, maximum annual SWE (mm per year) and maximum input (mm per time step) were tested for correlation with the annual averages of mean response time (each year averaged over the seven catchments) in order to distinguish between landscape controls on catchment hydrologic response and the influence of climatic fluctuations on intra-catchment variability. We also calculated the runoff ratios for each catchment (averaged over 12 years) and each year (averaged over seven catchments) and tested for correlation with the corresponding mean response times.

3. Results

3.1. Catchment Hydrology

[23] Annual elevation-weighted precipitation for LTC over the 12 years of simulation period averaged 790 mm and was 110 mm less compared to the 1961–1990 base period. The highest amount of precipitation and melt water entered the catchments in 1997 with an average of 960 mm among all catchments; 2001 had the least amount of input with an average of only 621 mm (Figure 3a). The timing and intensity of inputs varied from year to year but the average range among catchments was only 17 mm per year (BUB 788 mm, UTC 805 mm). The interannual variability in precipitation was much greater and hence more important than the intercatchment variability of the precipitation and melt inputs among the seven catchments.

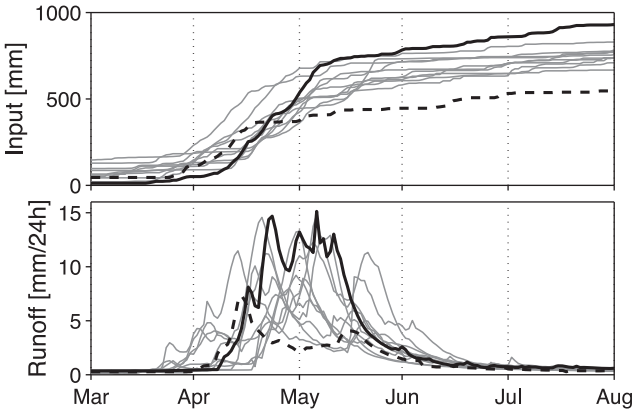

Figure 3. (a) Accumulated input (rainfall and snow melt) and (b) variations in discharge from 1996 to 2009. Year with max SWE (1997) denoted by black, bold line, year with minimum SWE (2001) denoted by black, dashed line.

[24] Runoff peaks varied strongly from year to year, with up to 23 days between the annual maximum peaks and peak magnitudes ranging from 4.2 to 15.1 mm d^{-1} at LTC. Single peaks were the exception, and multiple peaks generally occurred between mid-April and late May (Figure 3b).

3.2. Catchment Transfer Functions

[25] Model results indicate strong differences in transfer functions (Figure 4a). The greatest differences in catchment response occurred over the first 10 to 15 day portion of the transfer function (Figure 4b), with fractions of the input leaving the catchments (response fraction) within the first 24 h ranging from 10.3% (LTC) to 4.4% (SPC) with an average of 7.6% over all seven catchments. Response fractions for all catchments declined after the first day and averaged 3.6% on the 10th day after an input and ranged from 4.3% in BUB to 3.0% in SPC. Sixty days after the input event, average runoff contribution decreased to 0.1% of the original input with variations among catchments from 0.05% for LTC to 0.25% for SPC (Figure 4c). After 132 days, nearly all inputs left the catchments with runoff comprising less than 0.01% per day of original input. On average, a single precipitation or snowmelt input sustained runoff in the streams for about 132 days. The shortest complete transfer function was LSC (96 days), while LTC and SUN both maintained runoff for 153 days. Catchments with greater early response proportions do not necessarily maintain higher response through the season. For example SPC relatively low early response fractions but greater response than SUN by day 6 and greater than the other catchments by day 14. Whereas the daily SUN water contributions after 14 days exceed those of the other catchments, it still lags behind in total amount of water that has

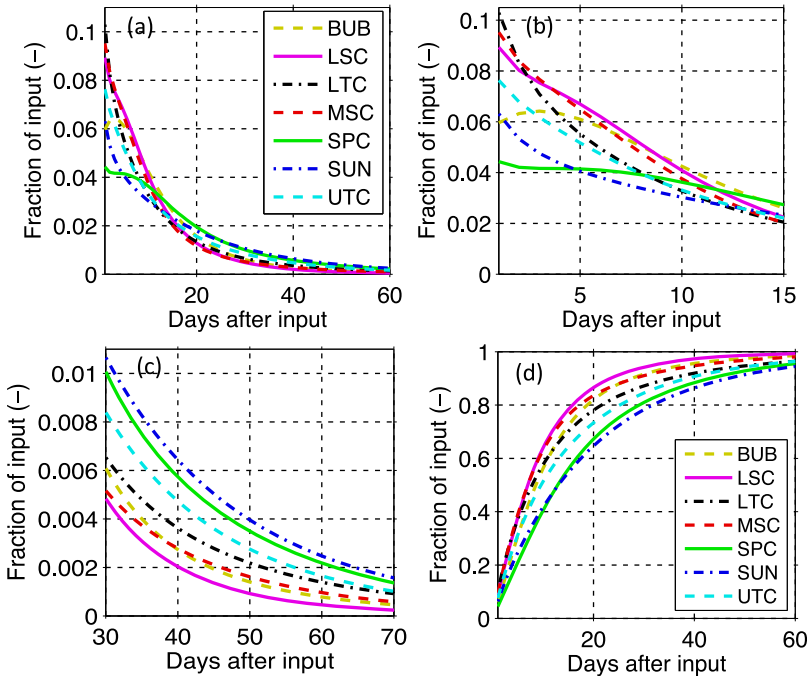

Figure 4. (a) Transfer functions for each catchment averaged over 12 simulated years; the *y* axis denotes the fraction of the input that left the watershed at a certain day; (b) short term behavior of the transfer functions (first 15 days); (c) long term (base flow) behavior of the transfer functions (days 30 through 70). Note the order of magnitude difference on the *y* axis as compared to the remaining panels; (d) cumulative distribution transfer functions for each catchment averaged over the 12 year simulation period; the *y* axis denotes the fraction of an input that left the watershed by a certain time (*x* axis); the steeper the curve at short times, the faster the precipitation to runoff response; an elevated curve later on indicates higher base flow contributions.

left the outlet in the remaining catchments and remains lower for the later parts of the transfer function. The cumulative transfer functions (Figure 4d) show that on average 20.6% of an input has left the catchments as streamflow after only 3 days, with individual catchments ranging from 12.8% (SPC) to 25.7% (LTC). After 9 days an average of 50% of the effective precipitation has left the catchments, with a maximum of 59.9% for LSC and a minimum of 37% for SPC. After 35 days an average of 90% of the input has left the catchments, ranging from 96.1% in LSC to 82.9% in SUN. After 85 days 99% of the original input has left the catchments.

[26] Averaged over the 12 years of simulation, mean response time for the seven catchments ranged from 9.56 days for LSC to 18.67 days for SPC, with the average of all catchments being 13.72 days (Table 2). Average Nash-Sutcliffe efficiencies across catchments ranged from 0.80 to 0.90.

3.3. Annual Transfer Functions

[27] The averaged transfer functions for each year of the 12 year simulation period (averaged over seven catchments for each year) exhibit strong differences (Figure 5a for averaged transfer functions and Figure 5b for the averaged cumulative transfer functions). The input was greatest in 1997 and smallest in 2001 (highlighted in Figure 5 as solid black line and dashed black line, respectively). The mean response times for each year averaged over the seven catchments ranged from 7.16 days in 2006 to 24.95 days in 2001 (Table 3). Average Nash-Sutcliffe efficiencies across years ranged from 0.72 to 0.92.

Table 2. Modeled Mean Response Times for the Seven TCEF Catchments, Averaged Over the 12 Simulated Years[a]

	BUB	LSC	LTC	MSC	SPC	SUN	UTC
Days	13.23	9.56	11.00	10.72	18.67	18.27	14.56

[a]Response times are in days.

3.4. Landscape Analysis

[28] The means and medians for slope (SLP), distance from creek (DFC), gradient to creek (GTC) and hillslope power (HP) for all seven catchments indicate an identical ranking for the catchments (i.e., the smallest mean corresponds to the smallest median and the largest mean to the largest median (Table 4)). Means and medians for convergence (CON) differ in sign, denoting slight convergence in the median but small divergence in the mean. The strongest departure between mean and median was evident for local input (LI), with the mean exceeding the median by up to an order of magnitude. Maps for 8 of the 10 topographic parameters are shown in Figure 6.

[29] Both the Kolmogorov-Smirnov and the Kruskall-Wallis tests resulted in p values $<< 0.01$ and highlight the significant difference for all the landscape metrics between the catchments.

[30] The strongest cross-correlations between the landscape metrics for LTC are correlations between SLP and

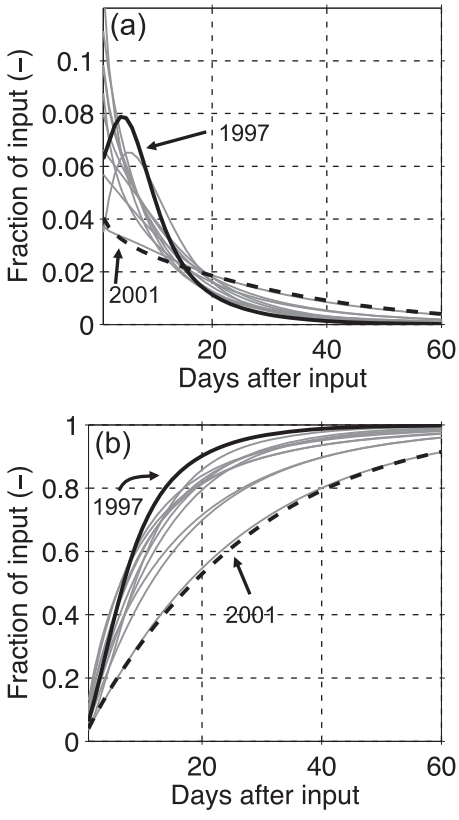

Figure 5. (a) Transfer functions and (b) cumulative distribution transfer functions averaged over all seven catchments for each of the 12 years simulated; the black solid lines denote the year with highest SWE (1997), the black dotted lines denote the year with lowest SWE (2001).

GTC ($r_p = 0.64$), INS and SLP ($r_p = -0.58$), GTC and DFC ($r_p = -0.43$) and SLP and DFC ($r_p = -0.30$). The metric with the weakest correlations was tree height (TH) with no correlation stronger than $r_p = \pm 0.08$. The cross-correlation matrix is shown in Figure 7.

3.5. Mean Response Time Correlations With Topographic Parameters

[31] There were no significant correlations between the landscape variables and modeled mean catchment response times, with the exception of mean convergence with $r_p = -0.94$ (Table 5). However, when the two catchments subjected to silvicultural harvesting (SUN and SPC) were omitted from the correlation, several significant relationships emerged. We excluded SUN and SPC from the correlation analysis because the silvicultural treatments and harvesting of more than 30% of the catchment areas have wide-ranging effects on hydrological processes [*Bosch and Hewlett*, 1982; *Stednick*, 1996]. We focus our analysis of landscape variables on the five remaining catchments and discuss the behavior of SUN and SPC in detail in the section 3.6.

[32] The correlations for both the mean and median for the majority of the landscape parameters were equally strong (Table 5). However, both LI and RB showed strong differences in mean and median in the correlations with mean response time, with the medians showing the stronger/significant correlations. The distributions for both LI and RB are highly positively skewed. We thus focus on the medians because they are more representative of the distributions of LI and RB than the arithmetic mean, which is more susceptible to extreme outliers and skewness.

Table 4. Topographic Parameters for Each Catchment[a]

	BUB	LSC	LTC	MSC	SPC	SUN	UTC
			SLP (°)				
Mean	6.5	9.5	8.0	8.6	9.5	6.5	5.4
Median	5.3	8.3	6.3	8.1	8.6	5.1	4.0
			CON (%)				
Mean	−0.020	−0.016	−0.014	−0.013	−0.029	−0.032	−0.026
Median	0.344	0.601	0.511	0.550	0.712	0.256	0.231
			DFC (m)				
Mean	575	452	545	491	440	691	714
Median	515	396	466	439	394	642	614
			GTC (−)				
Mean	0.135	0.168	0.142	0.140	0.153	0.104	0.088
Median	0.104	0.149	0.119	0.140	0.145	0.094	0.072
			LI (m^2)				
Mean	6511	7280	7343	8480	6645	10,546	10,058
Median	3345	2357	2403	2367	1695	3326	3510
			HP (−)				
Mean	517	595	547	594	552	563	450
Median	215	313	248	310	238	221	191
			RB (−)				
Mean	0.69	0.045	0.465	0.053	0.115	0.044	0.043
Median	0.022	0.028	0.028	0.031	0.043	0.024	0.024
			TH (m)				
Mean	3.65	3.01	3.03	3.10	2.51	2.41	3.83
			INS (kWh yr^{-1})				
Mean	3392	3428	3418	3442	3463	3401	3427
Median	3419	3461	3443	3461	3487	3430	3450
			GEO (% Catchment Area)				
Sandstone	92.9	56.2	70.3	54.7	31.2	91.4	97.6
Wolsey shale	0	19	9.8	19.9	26.7	0	2.2
Monzonite	0	15.3	10.8	23.8	40.4	0	0

[a]Means and medians with percent of catchment area for geology. The median for TH was 0 and is not shown here.

Table 3. Modeled Mean Response Times for Each Individual Year, Averaged Over the Seven Catchments[a]

	1996	1997	1998	1999	2000	2001	2002	2005	2006	2007	2008	2009
Days	12.66	9.76	24.73	13.22	13.81	24.95	17.44	11.95	7.16	10.44	10.13	8.34

[a]Response times are in days.

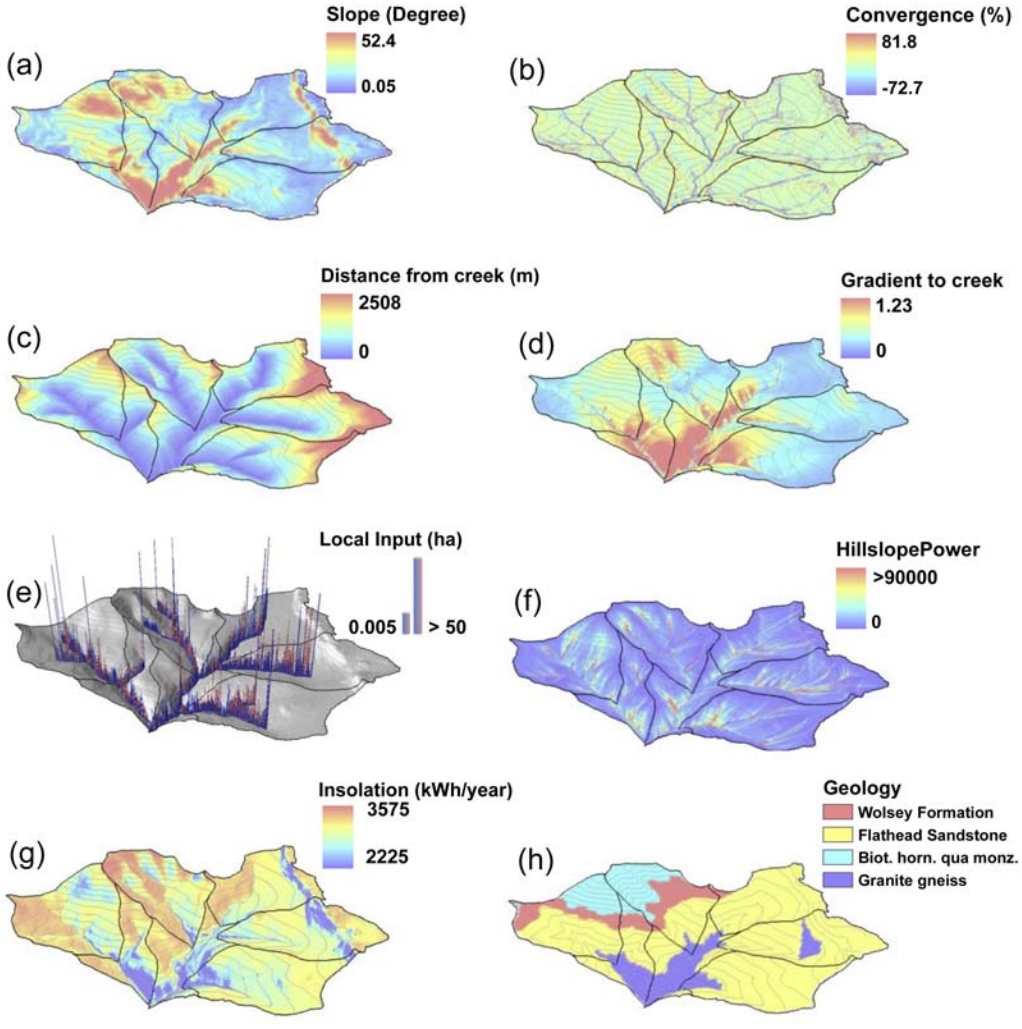

Figure 6. Map representation of topographic parameters for seven TCEF catchments, including (a) slope, (b) convergence, (c) distance from creek, (d) gradient to creek (e) local input, (f) hillslope power, (g) insolation, and (h) geologic strata.

[33] The landscape variables plotted versus the mean response times of the different catchments indicate strong correlations for multiple landscape metrics (Figures 8 and 9). Although excluded from the correlation analysis, SPC and SUN are displayed in Figure 8 for completeness.

3.6. Mean Response Time Correlations With Climatic Variables

[34] Maximum elevation weighted SWE for LTC ranged from 282 mm in 2001 to 467 mm in 1997 (Table 6). The correlation with the annually averaged mean response times was significant ($r_p = -0.82$); the greater the snowpack was during a given year, the faster the mean response time averaged among all seven catchments (Figure 10). From the input intensities for temporal windows ranging from 1 to 21 days, the period with the greatest intensity over a 13 day moving window exhibited the strongest and most significant correlation with mean annual response time ($r_p = -0.76$). Maximum input intensities over 13 days ranged from 16.3 mm d^{-1} in 2001 and 1998 to 23.1 mm d^{-1} in 1997, resulting in 211.9 mm in 13 days in 2001 and 1998 to 300.3 mm in 1997.

3.7. Mean Response Time Correlations With Runoff Ratios

[35] There was a strong, significant correlation between mean response time and the runoff ratio for each catchment (Figure 11a) with $r_p < -0.96$ for both the modeled and measured runoff ratios, omitting SUN and SPC. Larger runoff ratios were generally associated with shorter mean response times. However, with SUN and SPC included the correlation decreased to $r_p = -0.74$ for observed runoff ratios and $r_p = -0.79$ for simulated runoff ratios. In contrast, there was no significant correlation for averaged annual response times and annual runoff ratios ($r_p = 0.41$ for the observed runoff ratios and $r_p = -0.42$ for the simulated runoff ratios) (Figure 11b).

4. Discussion

[36] The influence of topographic structure, geology, vegetation distribution and climate on hydrologic response is of intense interest. However, the independent and combined influences of climatic variability and landscape characteristics on stream response remain poorly understood.

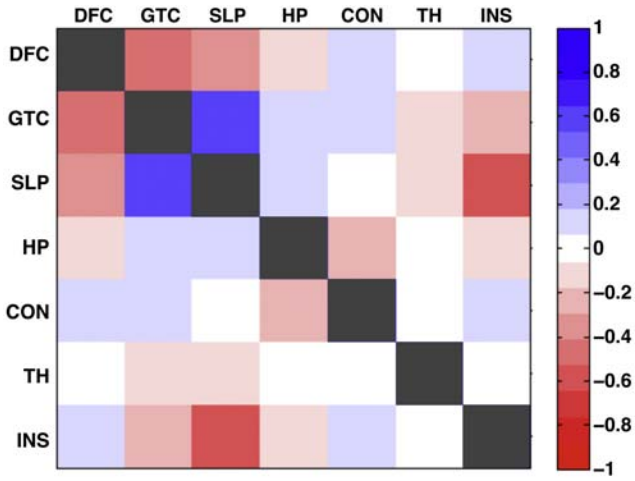

Figure 7. Cross-correlation matrix (Pearson's correlation coefficient) between seven landscape metrics. Correlations were calculated on a grid cell-to-grid cell basis using each 1 m grid cell across coverage. Blue colors indicate positive correlations, red colors indicate negative correlations. The gray diagonal is the correlation of a landscape metric with itself.

We calculated mean response times, the average time it takes for a liquid water input from the moment it hits the ground surface to leave the catchment through the outlet, for both catchment averages and annual averages for seven catchments and 12 years. We analyzed the seven TCEF subcatchments for a total of nine landscape structure metrics that can all be derived from airborne LIDAR data, including tree height distributions and potential solar insolation. We also calculated fractions of geologic strata types for each catchment. In addition to stationary topographic metrics we analyzed nonstationary climatic metrics, derived from two NRCS SNOTEL sites within TCEF. These data allowed us to independently examine the influence of both topography and climate on modeled mean response time. The following discussion focuses on the five more pristine catchments BUB, LSC, LTC, MSC, and UTC. The two catchments, which were subjected to silvicultural treatments, SUN and SPC, will be discussed separately.

Table 5. Correlations Between the Modeled Mean Response Time and the Topographic Parameters for Catchment Averages over 7 and 5 Catchments Without SPC and SUN[a]

	All Catchments ($n = 7$)			W/o SUN and SPC ($n = 5$)		
SLP	Mean	Median		Mean	Median	
r_p	0.25	−0.23		−1.00[b,c]	−0.95[b,c]	
CON	Mean	Median		Mean	Median	
r_p	−0.94	−0.20		−0.87	−1.00[b,c]	
DFC	Mean	Median		Mean	Median	
r_p	0.34	0.42		0.95[b]	0.98[b,c]	
GTC	Mean	Median		Mean	Median	
r_p	−0.43	−0.32		−0.91[b]	−0.97[b,c]	
LI	Mean	Median		Mean	Median	
r_p	0.30	0.10		0.46	0.96[b,c]	
HP	Mean	Median		Mean	Median	
r_p	−0.28	−0.64		−0.95[b]	−0.93[b]	
RB	Mean	Median		Mean	Median	
r_p	0.46	0.27		0.07	−0.81	
TH	Mean			Mean		
r_p	−0.45			0.97[b,c]		
INS	Mean	Median		Mean	Median	
r_p	0.11	0.10		−0.39	−0.53	
GEO	Shale	Sandst.	Monz.	Shale	Sandst.	Monz.
r_p	−0.13	0.04	0.11	−0.89[b]	0.95[b]	−0.83

[a]Significance level for a two-tailed test with $n = 7$ and $\alpha = 0.01$ equals $r_p = \pm 0.87$, and with $\alpha = 0.05$ the significance level equals $r_p = \pm 0.75$.
[b]Significance level for a two-tailed test with $n = 5$ and $\alpha = 0.05$ equals $r_P = \pm 0.88$.
[c]Significance level for a two-tailed test with $n = 5$ and $\alpha = 0.01$ equals $r_P = \pm 0.96$.

4.1. What Are the Interdependencies of the Selected Landscape Metrics?

[37] Comparing the effect of different landscape metrics on hydrologic response raises the question about redundancies in the chosen metrics, i.e., whether two seemingly different metrics are effectively expressing the same phenomenon due to strong cross correlation. To date, a few studies focusing on landscape evolution have addressed cross correlations between catchment characteristics, most notably the effect of vegetation on landscape metrics such as drainage density [*Istanbulluoglu and Bras*, 2005] and the effect of drainage networks structure on vegetation distribution and plant water stress [*Caylor et al.*, 2004]. To our knowledge no studies have calculated grid cell based correlations of LIDAR derived topographic metrics. We investigated metric interdependencies by calculating cross correlation between metrics for which values existed for each cell.

[38] The correlation matrix calculated for LTC shows no correlations stronger than $r_p = \pm 0.64$ and only four of the 21 correlations are stronger than $r_p = \pm 0.30$ (Figure 6). However, some redundancy in the chosen landscape metrics is apparent with the most obvious being SLP (the slope angle of an individual cell based on the surrounding eight cells) and GTC (the gradient integrated over the flowpath from a particular cell to the stream). Based on these definitions SLP and GTC are not necessarily correlated with each other (e.g., a low angle cell sits on top of a steep flowpath). However, Figure 6 indicates that the steepest local slopes of LTC correspond with the steepest gradients. This also explains the negative correlations between DFC-GTC and DFC-SLP: in general slope and gradients at TCEF increase toward the outlet of each catchment and are therefore correlated with DFC.

[39] The negative correlation between SLP and INS is a result of how slope and insolation interact. Insolation is a function of aspect and slope. In general south facing slopes have a higher insolation than north facing slopes. However, on south facing hillslopes a steeper slope increases solar insolation, whereas a steeper slope on north facing areas leads to a decrease in insolation.

[40] *Florinsky and Kuryakova* [1996] reported correlations between vegetation type and topographic metrics, especially those affecting solar insolation. However, no correlations between TH and landscape metrics were observed at TCEF.

[41] Due to the lack of strong cross correlations between the landscape variables, we can assume that potential significant correlations between landscape variables and mean response times are the result of individual but interacting

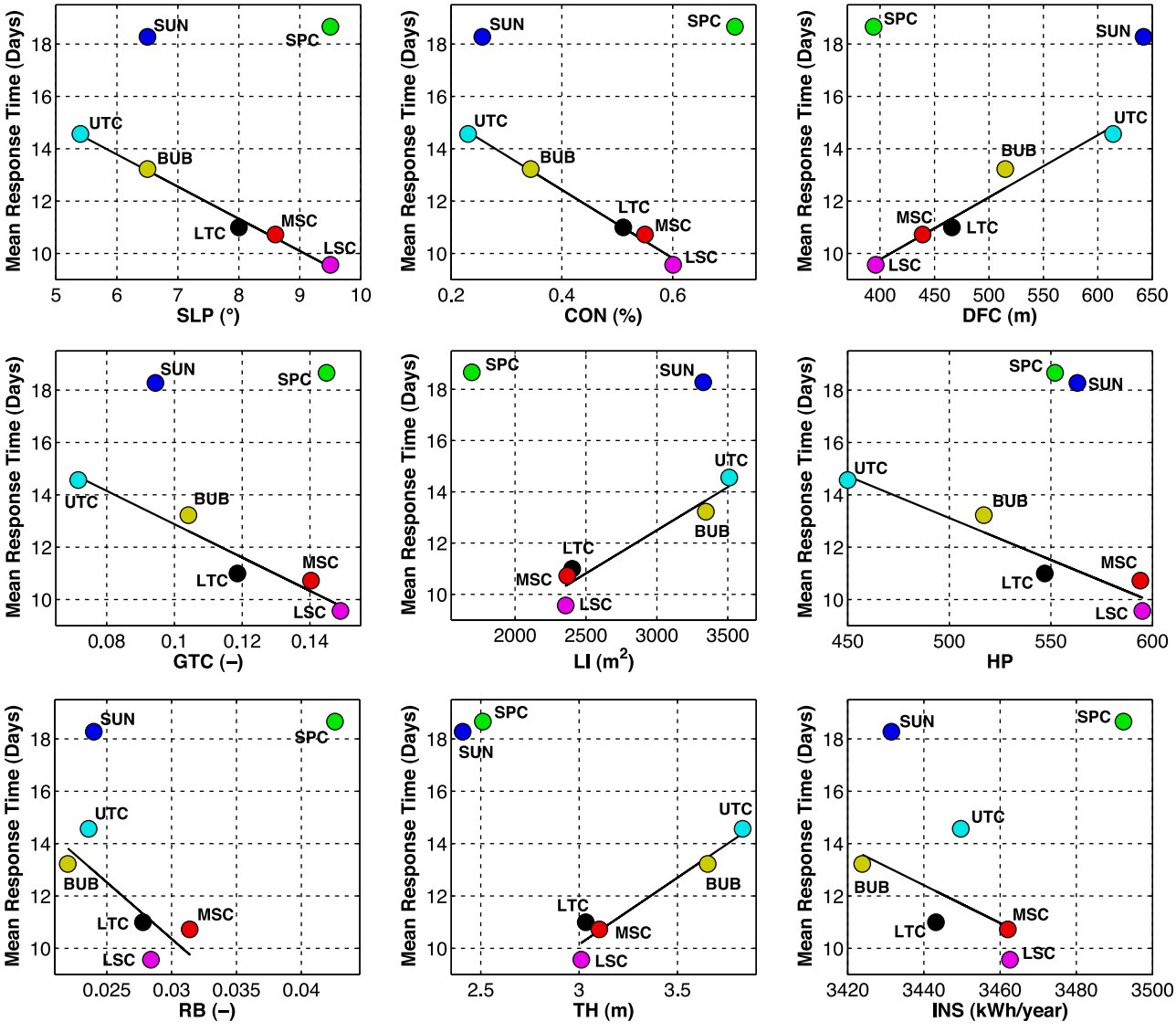

Figure 8. Regressions between mean response time (days) and topographic parameters. SUN and SPC have been excluded from the regressions but are shown for completeness; each symbol represents the averaged mean response time for one catchment over 12 years.

effects, rather than a manifestation of one effect (one variable) in several variables.

4.2. How Does Topography Explain the Observed Differences in Average Catchment Response Times?

[42] For a majority of the landscape metrics considered in this study, we found strong linear relationships with mean response time (Figures 8 and 9). SLP and GTC both exhibited a strong negative correlation with mean response time. The similar strength of the correlations is a result of the strong correlation of the two metrics with each other. These results confirm the greater the slope or the gradient to creek the faster the mean response time.

[43] Conversely, greater DFC increases the mean response time, which is consistent with geomorphic instantaneous unit hydrograph theory [*Gupta et al.*, 1980; *Rodriguez-Iturbe and Valdes*, 1979]. Simply stated, the greater

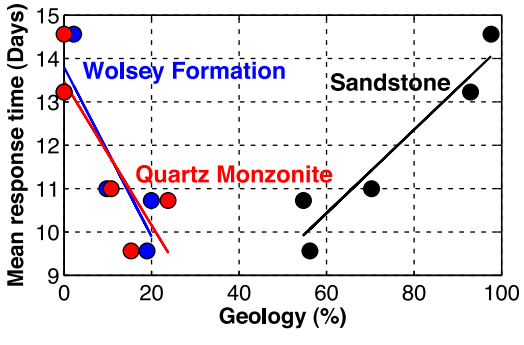

Figure 9. Regressions between the mean response time for the five catchments (BUB, LSC, LTC, MSC, and UTC) and the percentage of each geologic strata present in each catchment.

Table 6. Maximum SWE Elevation Weighted for LTC and Maximum Calculated Input Intensities Over 13 Consecutive Days and r_p With the Averaged Response Time for Each Year[a]

Year	Max SWE Elevation Weighted (mm)	Max Input Intensity Over 13 Days (mm d^{-1})
1996	387	21.0
1997	467	23.1
1998	306	16.3
1999	319	19.2
2000	364	16.9
2001	282	16.3
2002	337	17.6
2005	375	17.2
2006	446	22.8
2007	352	20.5
2008	395	18.2
2009	408	21.5
Correlations with mean response time	−0.82	−0.76

[a]Significance level for $n = 12$ and $\alpha = 0.01$ equals $r_p = \pm 0.71$.

the distances that water or input signals must travel, the longer it takes them to reach the catchment outlet. The positive relationship between DFC and mean response time is likely amplified by the slight negative correlation between SLP/GTC and DFC: short flow paths tend to have steeper gradients while longer flow paths are often associated with gentler gradients (Figures 6 and 7).

[44] The inverse relationship found for LI (positive correlation with response time) and CON (negative correlation with response time) seems counterintuitive at first since both metrics are a measure of flow accumulation. The results for local input are consistent with the findings of *Jencso et al.* [2009] who found a strong relationship between LI size and the duration of a hydrologic hillslope-riparian area-stream hydrologic connection. *Jencso et al.* [2009, 2010] reported that a larger LI does not necessarily mean that more water gets transported from the hillslope to the streams at any

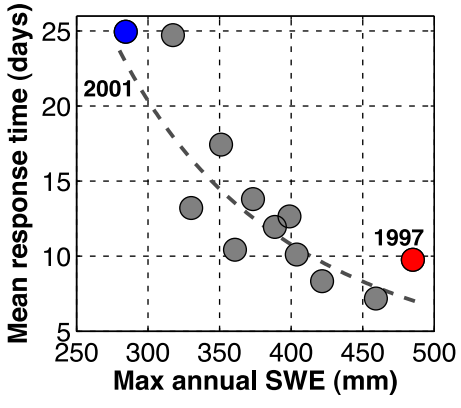

Figure 10. Relationship between maximum annual SWE (mm) and mean response time (days) averaged over all seven catchments for each of the 12 years of simulation. The gray dashed line is a power law regression (R2 = 0.75). The higher the maximum annual SWE, the faster the response time. The blue symbol denotes the year with lowest SWE (2001), the red symbol denotes the year with highest SWE (1997).

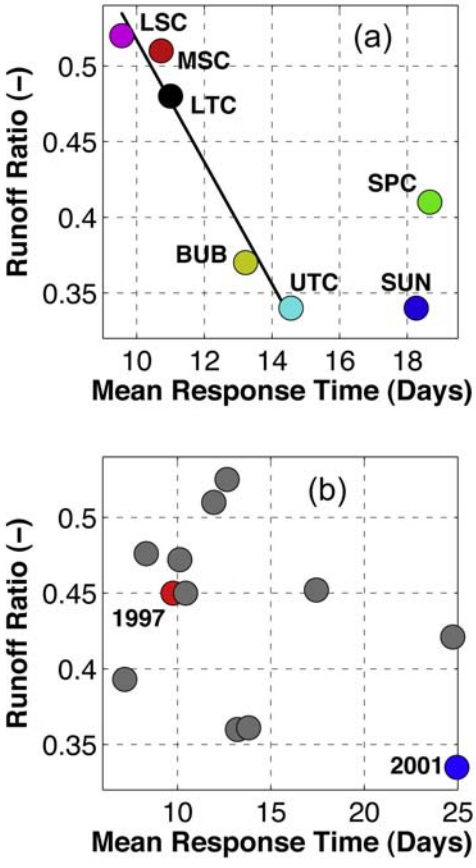

Figure 11. (a) Mean response time for catchment averages plotted against catchment runoff ratios (each point represents an average over 12 years). Omitting SUN and SPC there is a strong negative correlation, with smaller runoff ratios associated to longer mean response times; (b) Mean response time for annual averages plotted against annual averaged runoff ratios (each point represents an average of 7 catchments for each year) with no significant correlation. The blue symbol denotes the year with lowest SWE (2001), the red symbol denotes the year with highest SWE (1997).

given time but rather that larger LI hillslopes contribute for a longer period of time than smaller size LIs. It is the longevity of the hillslope-stream connection that is mediated by LI and not how fast water is being delivered to the stream. Note that LI is the UAA size for grid cells bordering the stream, whereas CON was calculated for every grid cell in each catchment, resulting in a metric that is more suitable to assess overall catchment concavity than LI, which describes overall hillslope size and connectivity potential for near-stream cells. Comparing CON and LI we found a significant negative correlation between the means and medians of the two metrics at the catchment scale, with $r_p = -0.98$: the larger the mean and median local input to the stream, the smaller the overall catchment convergence. A higher catchment convergence means that all catchment grid cells have more neighboring cells draining into them than catchments with a smaller convergence. CON can hence be considered a measure of catchment complexity or dissection, with less convergent catchments being less dissected, resulting in larger hillslope UAAs while more convergent catchments

exhibit a higher degree of topographic dissection. For instance, the most convergent catchments at TCEF are also the steepest catchments. Topographic dissection increases at TCEF in a downstream direction. UTC, at the headwaters of TCEF, consists of large, relatively planar hillslopes with long flowpath lengths and can be considered relatively simple in terms of topographic dissection. However, in a downstream direction, slopes increase, the stream becomes more incised, the riparian areas narrow, flowpath lengths become shorter, local input decreases, and convergence increases leading to greater landscape dissection.

[45] Another metric describing the potential for water accumulation and the associated potential energy is hillslope power (HP). In contrast to CON, HP is highly related to LI. In addition to upslope area, HP incorporates slope and therefore the energy gradient associated with this water. Therefore, HP can be related to the potential rate of water movement. This may only apply to saturated soils and not necessarily to unsaturated soils, where additional forces (e.g., matric potential) influence water movement. However, soils at TCEF are saturated or near saturation for periods during snowmelt [*Jencso et al.*, 2009]. The correlation between HP and mean response time is negative, a higher HP was correlated with a lower mean response time (similar to SLP and GTC).

[46] The final topographic metric, riparian buffering (RB), is also related to LI in that it is the dimensionless ratio of riparian area and the corresponding hillslope area that drains into it (riparian area/hillslope area). Its correlation with mean response time is negative ($r_p = -0.81$ for the median) but below the significance threshold, the correlation for the mean is even less strong ($r_p = 0.07$, Table 5). A negative correlation indicates that higher riparian buffering potentials are associated with shorter mean response times, a result that seems counterintuitive. One would expect a greater potential for volumetric buffering as indicated by *McGlynn and McDonnell* [2003], *McGlynn and Seibert* [2003] and *Jencso et al.* [2010] with more riparian area in relation to hillslope area. In fact, *Jencso et al.* [2010] observed a logarithmic relationship between riparian buffering potential and the turnover half-life time for the groundwater stored in riparian areas (the time it takes to replace 50% of riparian water with water from an adjacent hillslope). Based on the findings of *Jencso et al.* [2010], a positive correlation between RB and mean response time would have been expected. However, RB is a good example why it is important to differentiate between mean residence time (replacement of riparian water by hillslope water) and mean response time (displacement of water in the saturated riparian zone by hillslope water).

4.3. Do Vegetation and Energy Availability Have an Impact on Mean Response Times?

[47] Vegetation affects watershed hydrology in many ways and at all times during the hydrologic year. Two important hydrologic processes affected by vegetation in snow-dominated catchments during the winter include snow interception and subsequent sublimation from the canopy [*Hedstrom and Pomeroy*, 1998; *Pomeroy et al.*, 2002; *Pomeroy et al.*, 1998]. During the growing season, vegetation acts as loss mechanism for soil moisture because of evapotranspiration [*Rodriguez-Iturbe et al.*, 1999]. However, for snow-dominated systems, interception and sublimation are likely the dominant processes that affect mean response time at the annual scale.

[48] Our results indicate that tree height (TH) and mean response time are positively correlated ($r_p = 0.97$), with a greater TH leading to a longer mean response time (Table 5 and Figure 8). TH was calculated by incorporating all grid cells, including clear cuts, thins, parks, and cells absent of trees in forests, which reduced the estimated catchment average tree height considerably but is a better surrogate for "tree-biomass" for a given catchment in a lodgepole pine dominated landscape. Mean response time can be affected by vegetation and TH in various ways, most notably in the accumulation and melt of snow in snow dominated systems. Forests often accumulate less snow [*Woods et al.*, 2006], but they hold the snow longer than clearcut areas and parks [*Winkler et al.*, 2005]. This behavior is attributed to attenuated energy input to the subcanopy snowpack and enhanced canopy interception and sublimation. In hydrologic models attenuation of shortwave radiation by forest canopies is often calculated by incorporating LAI [e.g., *Wigmosta et al.*, 1994], with a greater LAI leading to less shortwave radiation penetrating the canopy, resulting in less energy to melt the subcanopy snowpack. LAI estimates in coniferous forests are often made through allometric relationships with tree height. *Keane et al.* [2005] established tree height-LAI relationships for TCEF for ground based LAI estimation methods and *Jensen et al.* [2008] found a linear relationship between LIDAR derived tree height and LAI for coniferous forests (among others consisting of pine and spruce species) in northern Idaho. Based on the relationship found by *Jensen et al.* [2008] and *Keane et al.* [2005], TH corresponds to a greater LAI and therefore increased potential to reduce incoming shortwave radiation received by the snowpack in forested areas, thus slowing down snowmelt and mean response time. The water input to the system as measured by the SNOTEL sites is potentially biased in that the SNOTEL stations are located in open areas and typically melt out earlier than forested sites due to differences in snowpack energy balances [*Woods et al.*, 2006]. Personal observations by the authors at TCEF during the last eight years corroborate that the forests hold snow longer than open areas. Therefore, the TH-mean response time relationship could be influenced by delayed melt in forests as compared to the SNOTEL sites.

[49] In addition to the potential effect of TH on snowpack energy balances, topographically mediated potential solar insolation also varies across the 7 catchments. Potential solar insolation (INS) is a function of aspect, slope, and geographic latitude and describes the incoming shortwave radiation for each grid cell accumulated over one year. In snow dominated catchments increased solar radiation can decrease snow accumulation by enhancing both sublimation of the snowpack and vegetation intercepted snowfall [*Jost et al.*, 2007; *Lopez-Moreno and Stahli*, 2008]. Therefore, INS can influence both the magnitude and timing of snowmelt. In general north facing slopes receive less incoming radiation, accumulate more snow, and release this water later in the melt period [*Murray and Buttle*, 2003]. This leads to a dampened yet sustained input through time, which increases mean response time. South facing catchments would exhibit the opposite behavior. Most catchments, however, contain a wide range of aspect and slope. Therefore,

mixtures of catchment landscape attributes can effectively work in opposition thereby muting the effect of INS. As expected, the correlations between mean response time and mean and median INS are negative (higher INS leads to shorter mean response times) but with $r_p = -0.39$ for the mean and $r_p = -0.53$ for the median, respectively, they are both below the 95% significance threshold. INS is the potential solar insolation on the ground surface and does not incorporate any attenuating factors, i.e., vegetation. The effective insolation that reaches the ground surface may differ significantly from the calculated potential solar insolation because of interception by the vegetation. The strong correlation between TH and mean response time highlights the importance of vegetation on hydrologic response and also explains why solar radiation input to the ground surface as single metric might be insufficient for prediction of hydrologic response.

4.4. What is the Role of Geology on Hydrologic Response?

[50] Bedrock geology can influence water chemistry [e.g., *Gardner and McGlynn*, 2009; *Newton et al.*, 1987; *Gardner et al.*, 2011] and the routing of water downslope and downstream [e.g., *Freer et al.*, 2002; *Onda et al.*, 2001].

[51] We evaluated the influence of geologic strata at TCEF to quantify the potential effect of different types of bedrock on mean response time. Strong, significant correlations between fraction of surficial bedrock geology and mean response time were observed for three of the four geologic layers at TCEF, with sandstone exhibiting the highest correlation, $r_p = 0.95$ (Table 5 and Figure 9). In contrast to the sandstone layer, correlations between mean response times and the shale and monzonite layers were negative. While sandstone is a sedimentary rock with relatively high hydraulic conductivities, both shale and monzonite (an igneous intrusive rock), have hydraulic conductivities several orders of magnitude lower than sandstone in unfractured conditions [*Freeze and Cherry*, 1979], likely leading to less recharge into deeper groundwater reservoirs. Potentially elevated seepage occurring into the sandstone relative to the shale and monzonite may reenter the shallow soil system and/or stream network further downslope. Because of longer travel times in the bedrock layer than in the (saturated) soil system, base flow contributions in catchments with greater sandstone fractions may be higher and mean response times longer. *Jencso and McGlynn*, [2011] found that the intersection of hillslopes greater than 0.5 ha with the sandstone layer extended flow duration curves for TCEF catchments. This is consistent with our findings that the sandstone fraction in a catchment is positively correlated with mean response time.

4.5. Can Intracatchment (i.e., Interannual) Variability be Explained by Climate Forcing?

[52] The transfer functions for both catchment averages over time (Figure 4) and annual averages of mean response time across catchments (Figure 5) exhibited considerable variability. While catchment averages of mean response time can be explained by topographic characteristics of each catchment (Figures 8 and 9), the question remains: what causes the differences observed in response time between the individual years (Figure 5)? Higher rainfall intensities generally lead to faster hydrologic response [*Montgomery et al.*, 1997], and antecedent moisture is often a key factor for low-intensity events [*Castillo et al.*, 2003; *Niehoff et al.*, 2002]. At TCEF, higher input intensities that are typically a combination of snowmelt and rainfall, lead to faster annual mean response times (Table 6). We evaluated input intensities for temporal windows ranging from one to 21 days. We selected the period with the greatest intensity for each temporal window and correlated them with catchment mean response times. For these input intensities, the correlation was strongest for the 13 day window ($r_p = -0.76$, Table 6). However, somewhat surprisingly the simple metric of maximum annual snow water equivalent (SWE) exhibited a slightly stronger correlation ($r_p = -0.82$, Table 6). A power law regression between maximum annual SWE and mean response time indicated that that 75% of the variability in annual mean response time could be explained by maximum annual SWE alone (Figure 10).

[53] Since mean response time was calculated for each input signal it is likely that the size of the snowpack affects response times by shifting soils from unsaturated to saturated, increasing hydraulic conductivity, increasing the saturated thickness (higher water tables), and increasing hydraulic gradients toward the stream. Greater SWE could also lead to a greater number of consecutive melt inputs to the ground (i.e., days with melt), increasing soil moisture for the next input and maintaining higher perched water tables above the bedrock-soil interface. This would suggest that both the input intensities and the duration of melt events have an effect on the rate of hydrologic response in snow-dominated systems.

4.6. What is the Relationship Between Mean Response Times and Runoff Ratios in the Context of Topographic and Climatic Variability?

[54] In our study, runoff ratios exhibited different behavior when they were calculated for catchment averages or annual averages. There was a strong negative relationship between runoff ratios and mean response time for catchment averages (Figure 11a). However, there was no visible pattern for annual runoff ratios versus annual mean response time (Figure 11b), suggesting that runoff ratios in a snowmelt dominated system like TCEF are determined by topography and not by climatic variability. This result is corroborated by nonsignificant relationships between maximum annual SWE and annual runoff ratios (Figure 12a) as well as annual precipitation amounts and annual runoff ratios (Figure 12b). This means that in general steeper catchments will have a higher runoff ratio compared to flatter watersheds but the ratio is independent of the amount of snowmelt. These results are counter to previous research, which indicated runoff ratios largely depended on local climate, i.e., the availability of energy and precipitation [*Arora*, 2002; *Budyko*, 1974; *Donohue et al.*, 2007; *Hewlett and Hibbert*, 1967; *Pike*, 1964; *Zhang et al.*, 2001].

[55] We can assume that independent of the actual input magnitudes the catchments wet up fairly quickly due to the large melt input in even the low-precipitation years. SWE magnitudes may therefore be secondary to topographic influences in determining runoff ratios. However, this does not contradict our finding that SWE impacts mean response

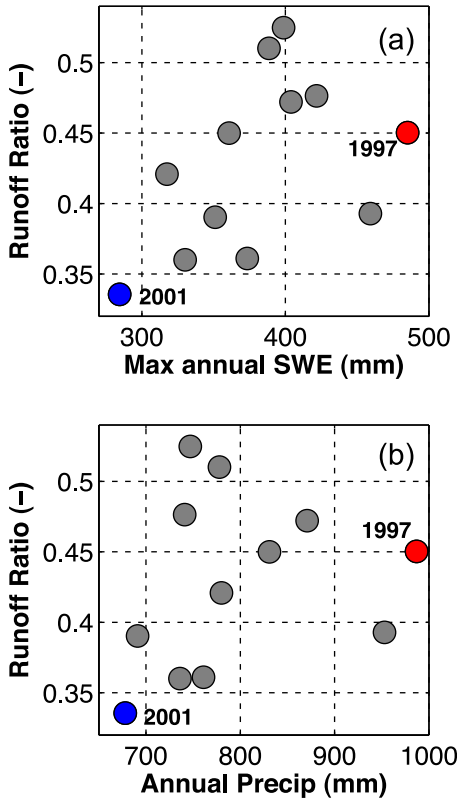

Figure 12. (a) Maximum annual SWE versus average annual runoff ratios, $r_p = 0.48$ and p value $= 0.11$. (b) Annual precipitation versus average annual runoff ratios, r_p and p value $= 0.47$. Both correlations are nonsignificant.

times. While response time is controlled by input intensities over longer time periods, annual runoff ratios appear to be mostly independent of max SWE and max input intensities due to the large magnitude of snowmelt events and the effect of ET and other melt/precipitation characteristics. These results suggest that even during small melt events, the velocity of subsurface flow depends mostly on the topography of each catchment, especially slope (i.e., Darcy's law), assuming homogenous soils with homogenous hydraulic conductivities across TCEF.

4.7. What Explains the Different Behavior of SUN and SPC?

[56] We excluded both the SUN and SPC catchments initially because of the silvicultural treatments in 2001/2002 and the potential treatment impact on the hydrologic cycle. Many studies have focused on the effect of silvicultural treatments and disturbances on hydrologic response [*Bosch and Hewlett*, 1982; *Cheng*, 1989; *DeBano*, 2000; *Miller*, 1984; *Swank and Douglass*, 1974] and most studies found increased water yield and increased stormflow following clear cutting.

[57] At TCEF, both SUN and SPC exhibited considerably longer mean response times than the other catchments and do not fit on any of the regressions shown in Figure 8. The harvests occurred in 2001 and 2002. We compared the mean response times of all catchments for both the pre and post logging periods (Table 7). The mean response times of SPC and SUN were longer than the mean response times of the remaining catchments for both the pre and post logging period, but more closely approached the response times of the other catchments in the post logging period. In general, mean response times decreased from the pre to post logging period for all catchments, which was likely caused by larger snowpacks in the post logging period, but the absolute decline is greatest for SPC and SUN. Therefore, patch cuts and thinned stands increased the responsiveness of the two managed catchments, however, they remained less responsive (longer mean response times) than the other catchments and less responsive than the landscape metric regressions would predict.

Table 7. Comparison of Mean Response Times for the Entire Simulation Period and the Pre- and Post-Logging Periods

	BUB	LSC	MSC	LTC	SPC	SUN	UTC	Average
1996–2009	13.23	9.56	11.00	10.72	18.66	18.27	14.56	13.72
Pre-logging	15.52	10.58	14.76	13.64	23.34	22.60	15.21	16.52
Post-logging	10.93	8.55	7.23	7.81	13.99	13.94	13.92	10.91

[58] Longer mean response times in SPC and SUN suggest that factors other than those derived from the digital elevation model, vegetation, and fractional geology must influence catchment runoff behavior in these two catchments. LIDAR data capture surface topography in great detail but are unable to detect subsurface topography. R. A. Payn et al. (Shift from topographic to subsurface structural controls on spatial patterns of stream baseflow during seasonal recession, submitted to *Water Resources Research*, 2011) have shown that subsurface contributing area in TCEF may differ from the contributing area derived from LIDAR data during low-flow conditions. Also the fraction of geologic strata for each catchment does not reveal information about the dip of the layers, the thickness of the layers, nor the location of geologic transitions relative to runoff generation processes.

[59] SPC covers the full range of geologic variability in TCEF with four different geologic layers. The transition from Wolsey shale to Flathead sandstone in SPC coincides with a noticeable break in slope (Figures 6a and 6h). The forested and clearcut hillslopes transition into a wide, open park (meadow). This park area is one of the wettest sites in TCEF with water tables close to the surface even in the late summer when most of TCEF has already dried down. R. A. Payn et al. (submitted manuscript, 2011) analyzed spatial patterns of stream base flow generation at TCEF and found steady or increasing contributions relative to the overall LTC runoff for the spring visible at the shale – sandstone interface during the summer dry down period in 2006. R. A. Payn et al. (submitted manuscript, 2011) suggest extensive storage in the SPC ridge area, which would sustain a higher runoff in the summer base flow period and lead to longer mean response times. Interestingly, an equal transition in MSC/LSC from shale to sandstone does not produce visible springs or wet areas, suggesting differences in the stratigraphic transition between the two catchments.

[60] On the other hand, SUN comprises mostly sandstone with a small fraction of granite gneiss and does not

exhibit noticeable transitions that would favor the formation of springs. The most notable geologic feature in SUN is a fault line (Quartzite ridge fault) that dissects SUN east to west in approximately equal portions. Runoff generated on the catchment portions above the fault could infiltrate along the fault into deeper geologic layers and reenter the system further downstream as return flow, thus increasing hydrologic response times. The fault also runs through BUB and UTC. However, the areas above the fault in these two catchments are significantly less than in SUN.

[61] The tailing behavior of the transfer functions of SPC and SUN also suggests higher base flow contributions as compared to the remaining catchments, which may be a combined result of sustained groundwater contributions and reduced evapotranspiration (Figure 4c).

5. Conclusions

[62] The use of runoff transfer functions provides a simple tool for assessing the hydrologic response of catchments and relating differences in response to landscape structure and climate. Based on our correlations using modeled mean response time and variables of landscape structure and climate we conclude the following.

[63] 1. Differences in mean response time among five of the TCEF catchments were caused by differences in landscape structure. There were no strong cross correlations among the TCEF landscape variables, suggesting that the observed correlations are not just the effect of one or two variables superimposed onto the others. However, it is intriguing that metrics that are seemingly independent from each other show equally strong correlations with mean response time. This raises questions of how independent catchment characteristics are in fact related and form during landscape evolution.

[64] 2. Vegetation has an effect on mean response time most likely due to reduced snow accumulation, the shading of the subcanopy snowpack and the attenuation of solar radiation used to melt the snowpack.

[65] 3. The Sandstone layer at TCEF showed the strongest correlation with mean response time. Variable hydraulic conductivities of the geologic strata at TCEF potentially lead to differing recharge rates into deeper groundwater layers, which also affected mean response time.

[66] 4. Interannual variability in mean response time was a result of variable climatic conditions, i.e., the maximum amount of annual snow water equivalent and differences in melt intensities.

[67] 5. The two apparent outliers SPC and SUN suggest controls on hydrologic response in these watersheds other than metrics of surface topography, i.e., metrics than can be derived from digital elevation models. Geology was likely responsible for this unexpected behavior. However, we were unable to ultimately answer the question of why the two catchments show hydrologic response that does not fall in line with the relationships established for the other five catchments.

[68] 6. For these snow dominated systems runoff ratios were largely a function of topography. This means that in general steeper catchments had higher runoff ratios compared to flatter watersheds. The runoff ratio was independent of the amount of snowmelt.

[69] Some of the correlations shown in this study are very strong and suggest that one single metric explains catchment runoff behavior (e.g., SLP and CON with an $r_p = -1.00$). However, we emphasize that catchment heterogeneity is too complex to reduce the governing factors of hydrologic response to individual landscape structural metrics. It is rather the interaction of several metrics that ultimately determines how a watershed responds to a precipitation input.

[70] We tested the transfer function rainfall-runoff modeling framework in a snowmelt-dominated system of the northern Rocky Mountains. Future applications of the model and analysis approach could involve comparisons of catchments in other places to test whether the relationships we established at TCEF also hold for different landscapes, climatic settings, and scales.

[71] **Acknowledgments.** This study was funded by NSF grants EAR-0943640 to Marshall and McGlynn, EAR-0837937 to McGlynn, EAR-0838193 to Emanuel through the Department of Geology at Appalachian State University, and the Inland Northwest Research Alliance (INRA). The authors would like to thank the U.S. Department of Agriculture, Forest Service, Rocky Mountain Research Station for providing runoff data and Kevin McGuire for providing his TRANSEP code.

References

Arora, V. K. (2002), The use of the aridity index to assess climate change effect on annual runoff, *J. Hydrol.*, *265*(1–4), 164–177.

Beven, K. J., and P. C. Young (1988), An aggregated mixing zone model of solute transport through porous media, *J. Contam. Hydrol.*, *3*, 129–143.

Böhner, J., and O. Antonic (2009), Land-surface parameters specific to topoclimatology, in *Geomorphometry: Concepts, Software, Applications, Dev. Soil Sci.*, vol. 33, edited by T. Hengl and H. I. Reuter, pp. 195–226, Elsevier, Amsterdam.

Bosch, J. M., and J. D. Hewlett (1982), A review of catchment experiments to determine the effect of vegetation changes on water yield and evapotranspiration, *J. Hydrol.*, *55*(1/4), 3–23.

Budyko, M. I. (1974), *Climate and Life*, Academic, New York.

Burt, T. P., and D. P. Butcher (1985), Topographic controls of soil-moisture distributions, *J. Soil Sci.*, *36*(3), 469–486.

Castillo, V. M., A. Gomez-Plaza, and M. Martinez-Mena (2003), The role of antecedent soil water content in the runoff response of semiarid catchments: A simulation approach, *J. Hydrol.*, *284*(1–4), 114–130.

Caylor, K. K., T. M. Scanlon, and I. Rodriguez-Iturbe (2004), Feasible optimality of vegetation patterns in river basins, *Geophys. Res. Lett.*, *31*, L13502, doi:10.1029/2004GL020260.

Cheng, J. D. (1989), Streamflow changes after clear-cut logging of a pine beetle-infested watershed in southern British-Columbia, Canada, *Water Resour. Res.*, *25*(3), 449–456.

DeBano, L. F. (2000), The role of fire and soil heating on water repellency in wildland environments: A review, *J. Hydrol.*, *231*, 195–206.

Donohue, R. J., M. L. Roderick, and T. R. McVicar (2007), On the importance of including vegetation dynamics in Budyko's hydrological model, *Hydrol. Earth Syst. Sci.*, *11*(2), 983–995.

Dooge, J. C. I. (1959), A general theory of the unit hydrograph, *J. Geophys. Res.*, *64*(2), 241–256.

Dunne, T., and R. D. Black (1970), Partial area contributions to storm runoff in a small New England watershed, *Water Resour. Res.*, *6*(5), 1296–1311.

Emanuel, R. E., H. E. Epstein, B. L. McGlynn, D. L. Welsch, D. J. Muth, and P. D'Odorico (2010), Spatial and temporal controls on watershed ecohydrology in the northern Rocky Mountains, *Water Resour. Res.*, *46*, W11553, doi:10.1029/2009WR008890.

Farnes, P. E., R. C. Shearer, W. W. McCaughey, K. J. Hanson (1995), Comparisons of Hydrology, Geology and Physical Characteristics between Tenderfoot Creek Experimental Forest (East Side) Montana, and Coram Experimental Forest (West Side) Montana, *Final Rep. RJVA-INT-92734*. 19 pp. USDA Forest Service, Intermountain Res. Station, For. Sci. Lab., Bozeman, Mont.

Florinsky, I. V., and G. A. Kuryakova (1996), Influence of topography on some vegetation cover properties, *Catena*, *27*(2), 123–141.

Freer, J., J. J. McDonnell, K. J. Beven, N. E. Peters, D. A. Burns, R. P. Hooper, B. Aulenbach, and C. Kendall (2002), The role of bedrock topography on subsurface storm flow, *Water Resour. Res.*, *38*(12), 1269, doi:10.1029/2001WR000872.

Freeze, A. R., and J. A. Cherry (1979), *Groundwater*, Prentice Hall, Englewood Cliffs, N. J.

Gardner, K. K., and B. L. McGlynn (2009), Seasonality in spatial variability and influence of land use/land cover and watershed characteristics on stream water nitrate concentrations in a developing watershed in the Rocky Mountain West, *Water Resour. Res.*, *45*, W08411, doi:10.1029/2008WR007029.

Gardner, K. K., B. L. Mcglynn, and L. Marshall (2011), Quantifying watershed sensitivity to spatially variable N loading and the relative importance of watershed N retention mechanisms, *Water Resour. Res.*, *47*, W08524, doi:10.1029/2010WR009738.

Gupta, V. K., E. Waymire, and C. T. Wang (1980), A representation of an instantaneous unit-hydrograph from geomorphology, *Water Resour. Res.*, *16*(5), 855–862.

Hedstrom, N. R., and J. W. Pomeroy (1998), Measurements and modelling of snow interception in the boreal forest, *Hydrol. Processes*, *12*(10–11), 1611–1625.

Hewlett, J. D., and A. R. Hibbert (1967), Factors affecting the response of small watersheds to precipitation in humid areas, in *Forest Hydrology*, edited by W. E. Sopper and H. W. Lull, pp. 275–290, Pergamon, New York.

Holdorf, H. D. (1981), Soil resource inventory, Lewis and Clark National Forest, *Interim in Serv. Rep.*, Lewis and Clark Natl. For., For. Supervisor's Offi., Great Falls, Mont.

Hrachowitz, M., C. Soulsby, D. Tetzlaff, J. J. C. Dawson, and I. A. Malcolm (2009), Regionalization of transit time estimates in montane catchments by integrating landscape controls, *Water Resour. Res.*, *45*, W05421, doi:10.1029/2008WR007496.

Hrachowitz, M., C. Soulsby, D. Tetzlaff, I. A. Malcolm, and G. Schoups (2010), Gamma distribution models for transit time estimation in catchments: Physical interpretation of parameters and implications for time-variant transit time assessment, *Water Resour. Res.*, *46*, W10536, doi:10.1029/2010WR009148.

Istanbulluoglu, E., and R. L. Bras (2005), Vegetation-modulated landscape evolution: Effects of vegetation on landscape processes, drainage density, and topography, *J. Geophys. Res.*, *110*, F02012, doi:10.1029/2004JF000249.

Jakeman, A. J., and G. M. Hornberger (1993), How much complexity is warranted in a rainfall-runoff model?, *Water Resour. Res.*, *29*(8), 2637–2650.

Jencso, K. G., B. L. McGlynn, M. N. Gooseff, S. M. Wondzell, K. E. Bencala, and L. A. Marshall (2009), Hydrologic connectivity between landscapes and streams: Transferring reach-and plot-scale understanding to the catchment scale, *Water Resour. Res.*, *45*, W04428, doi:10.1029/2008WR007225.

Jencso, K. G., B. L. McGlynn, M. N. Gooseff, K. E. Bencala, and S. M. Wondzell (2010), Hillslope hydrologic connectivity controls riparian groundwater turnover: Implications of catchment structure for riparian buffering and stream water sources, *Water Resour. Res.*, *46*, W10524, doi:10.1029/2009WR008818.

Jencso, K. G., and B. L. McGlynn (2011), Hierarchical controls on runoff generation: Topographically driven hydrologic connectivity, geology, and vegetation, *Water Resour. Res.*, *47*, W11527, doi:10.1029/2011WR010666.

Jensen, J. L. R., K. S. Humes, L. A. Vierling, and A. T. Hudak (2008), Discrete return lidar-based prediction of leaf area index in two conifer forests, *Remote Sens. Environ.*, *112*(10), 3947–3957.

Jost, G., M. Weiler, D. R. Gluns, and Y. Alila (2007), The influence of forest and topography on snow accumulation and melt at the watershed-scale, *J. Hydrol.*, *347*(1–2), 101–115.

Jury, W. A. (1982), Simulation of solute transport using a transfer function model, *Water Resour. Res.*, *18*(2), 363–368.

Keane, R. E., E. D. Reinhardt, J. Scott, K. Gray, and J. Reardon (2005), Estimating forest canopy bulk density using six indirect methods, *Can. J. For. Res.*, *35*(3), 724–739.

Lopez-Moreno, J. I., and M. Stahli (2008), Statistical analysis of the snow cover variability in a subalpine watershed: Assessing the role of topography and forest, interactions, *J. Hydrol.*, *348*(3–4), 379–394.

Maloszewski, P., and A. Zuber (1982), Determining the turnover time of groundwater systems with the aid of environmental tracers: 1. Models and their applicability, *J. Hydrol.*, *57*(3–4), 207–231.

McGlynn, B. L., and J. J. McDonnell (2003), Quantifying the relative contributions of riparian and hillslope zones to catchment runoff, *Water Resour. Res.*, *39*(11), 1310, doi:10.1029/2003WR002091.

McGlynn, B. L., and J. Seibert (2003), Distributed assessment of contributing area and riparian buffering along stream networks, *Water Resour. Res.*, *39*(4), 1082, doi:10.1029/2002WR001521.

McGuire, K. J., D. R. DeWalle, and W. J. Gburek (2002), Evaluation of mean residence time in subsurface waters using oxygen-18 fluctuations during drought conditions in the mid-Appalachians, *J. Hydrol.*, *261*(1–4), 132–149.

Miller, E. L. (1984), Sediment yield and storm flow response to clear-cut harvest and site preparation in the Ouachita Mountains, *Water Resour. Res.*, *20*(4), 471–475.

Montgomery, D. R., W. E. Dietrich, R. Torres, S. P. Anderson, J. T. Heffner, and K. Loague (1997), Hydrologic response of a steep, unchanneled valley to natural and applied rainfall, *Water Resour. Res.*, *33*(1), 91–109.

Murray, C. D., and J. M. Buttle (2003), Impacts of clearcut harvesting on snow accumulation and melt in a northern hardwood forest, *J. Hydrol.*, *271*(1–4), 197–212.

Newton, R. M., J. Weintraub, and R. April (1987), The relationship between surface water chemistry and geology in the North Branch of the Moose River, *Biogeochemistry*, *3*(1–3), 21–35.

Niehoff, D., U. Fritsch, and A. Bronstert (2002), Land-use impacts on storm-runoff generation: Scenarios of land-use change and simulation of hydrological response in a meso-scale catchment in SW-Germany, *J. Hydrol.*, *267*(1–2), 80–93.

Nijssen, B., G. M. O'Donnell, A. F. Hamlet, and D. P. Lettenmaier (2001), Hydrologic sensitivity of global rivers to climate change, *Clim. Change*, *50*(1–2), 143–175.

Onda, Y., Y. Komatsu, M. Tsujimura, and J. Fujihara (2001), The role of subsurface runoff through bedrock on storm flow generation, *Hydrol. Processes*, *15*(10), 1693–1706.

Pacific, V. J., B. L. McGlynn, D. A. Riveros-Iregui, D. L. Welsch, and H. E. Epstein (2011), Landscape structure, groundwater dynamics, and soil water content influence soil respiration across riparian-hillslope transitions in the Tenderfoot Creek Experimental Forest, Montana, *Hydrol. Processes*, *25*(5), 811–827.

Pike, J. G. (1964), The estimation of annual run-off from meteorological data in a tropical climate, *J. Hydrol.*, *2*(2), 8.

Pomeroy, J. W., D. M. Gray, K. R. Shook, B. Toth, R. L. H. Essery, A. Pietroniro, and N. Hedstrom (1998), An evaluation of snow accumulation and ablation processes for land surface modelling, *Hydrol. Processes*, *12*(15), 2339–2367.

Pomeroy, J. W., D. M. Gray, N. R. Hedstrom, and J. R. Janowicz (2002), Prediction of seasonal snow accumulation in cold climate forests, *Hydrol. Processes*, *16*(18), 3543–3558.

Quinn, P. F., K. J. Beven, P. Chevallier, and O. Planchon (1991), The prediction of hillslope flow paths for distributed hydrological modelling using digital terrain models, *Hydrol. Processes*, *5*, 59–79.

Riveros-Iregui, D. A., and B. L. McGlynn (2009), Landscape structure control on soil CO_2 efflux variability in complex terrain: Scaling from point observations to watershed scale fluxes, *J. Geophys. Res.*, *114*, G02010, doi:10.1029/2008JG000885.

Rodriguez-Iturbe, I., and J. B. Valdes (1979), The geomorphologic structure of hydrologic response, *Water Resour. Res.*, *15*(6), 1409–1420.

Rodriguez-Iturbe, I., P. D'Odorico, A. Porporato, and L. Ridolfi (1999), On the spatial and temporal links between vegetation, climate, and soil moisture, *Water Resour. Res.*, *35*(12), 3709–3722.

Sherman, L. K. (1932), Streamflow from rainfall by the unit graph method, *Eng. News Rec.*, *108*, 501–505.

Smith, T. J., and L. A. Marshall (2010), Exploring uncertainty and model predictive performance concepts via a modular snowmelt-runoff modeling framework, *Environ. Model. Software*, *25*(6), 691–701.

Stednick, J. D. (1996), Monitoring the effects of timber harvest on annual water yield, *J. Hydrol.*, *176*(1–4), 79–95.

Swank, W. T., and J. E. Douglass (1974), Streamflow greatly reduced by converting deciduous hardwood stands to pine, *Science*, *185*(4154), 857–859.

Wallis, S. G., P. C. Young, and K. J. Beven (1989), Experimental investigation of the aggregated dead zone model for longitudinal solute transport in stream channels, *Proc. Inst. Civ. Eng. Part 2*, *87*, 1–22.

Weiler, M., B. L. McGlynn, K. J. McGuire, and J. J. McDonnell (2003), How does rainfall become runoff? A combined tracer and runoff transfer function approach, *Water Resour. Res.*, *39*(11), 1315, doi:10.1029/2003WR002331.

Western, A. W., R. B. Grayson, G. Bloschl, G. R. Willgoose, and T. A. McMahon (1999), Observed spatial organization of soil moisture and its relation to terrain indices, *Water Resour. Res.*, *35*(3), 797–810.

Wigmosta, M. S., L. W. Vail, and D. P. Lettenmaier (1994), A distributed hydrology—Vegetation model for complex terrain, *Water Resour. Res.*, *30*(6), 1665–1679.

Winkler, R. D., D. L. Spittlehouse, and D. L. Golding (2005), Measured differences in snow accumulation and melt among clearcut, juvenile, and mature forests in southern British Columbia, *Hydrol. Processes*, *19*(1), 51–62.

Woods, S. W., R. Ahl, J. Sappington, and W. McCaughey (2006), Snow accumulation in thinned lodgepole pine stands, Montana, USA, *For. Ecol. Manage.*, *235*(1–3), 202–211.

Zhang, L., W. R. Dawes, and G. R. Walker (2001), Response of mean annual evapotranspiration to vegetation changes at catchment scale, *Water Resour. Res.*, *37*(3), 701–708.

R. E. Emanuel, Department of Forestry and Environmental Resources,-North Carolina State University, 2217 Jordan Hall, Raleigh, NC 27695, USA.

L. A. Marshall, B. L. McGlynn, and F. Nippgen, Department of Land Resources and Environmental Sciences, Montana State University, 334 Leon Johnson Hall, Bozeman, MT 59717, USA. (fabian.nippgen@msu.montana.edu)